doi:10.36487/ACG_rep/1752_19_Liu

Bleeding characteristics and improved mechanism of self-flowing tailings filling paste with low concentration

Juanhong Liu *University of Science and Technology Beijing, China*

Ruidong Wu *University of Science and Technology Beijing, China*

Aixiang Wu *University of Science and Technology Beijing, China*

Shaoyong Wang *University of Science and Technology Beijing, China*

Abstract

In order to solve the bleeding problem of self-flowing tailings filling paste with low concentrations, the influences of the dosage of special additives on the bleeding rate were investigated. The improving mechanism of special additives on the bleeding of tailings filling paste was studied by measuring the bleeding rate and compressive strength of the paste and analyzing the scanning electron microscope (SEM), energy dispersive spectrometer (EDS) and infrared spectroscopy (IR) of the hardened paste. The results show that when the paste concentration is 60%, the binder-to-tailings ratio is 1:6, and the dosage of special additive is 10%, the filling paste is not bleeding and the compressive strength of the hardened paste can increase by 43.5% at 3 days. A large amount of needle-like ettringite is generated in the hardened paste after adding the special additives, and the structure becomes denser. The special additives can effectively improve the bleeding of the filling paste and increase the compressive strength of the filling material at early age.

1 Introduction

With the increased mining depth, tailings filling mining is more widely used in most large mines in China. In this case, a decrease of the paste fill solids concentration is needed in order for a better transportation. However, decreasing the paste concentration often leads to the problematic high seepage water bleed rate. Thus, a new kind of material should be developed to satisfy low solids concentration in the conveying process, reduce the bleed rate of seepage water after entering the stope as well as increase its strength. The use of tailings for cemented filling can efficiently utilize all mine tailings and reduce environmental pollution and the cost of mine filling (Zhai et al., 2011). As grading is not required for tailings, the filling paste will have good conveying performance and high filling efficiency (Zhang et al., 2011; Fusi et al., 2012). However, at low solids concentration, high bleed water seepage rates will occur when the self-flowing tailings filling paste is deposited underground (Yong et al., 2011). The bleeding directly causes the shrinkage of fill, resulting in a decreased capacity in roof contacting and therefore affecting the stope safety. Moreover, the seepage also causes the pollution of underground roadway and increases the cost of water drainage.

The rheological properties and strength characteristics of cemented tailings filling paste were widely studied in over the past decade (Wu et al., 2012; Syrakos et al., 2013; Peyronnard and Benzaazoua, 2012; Fall et al., 2009), but little research has been done on the reduction mechanism of bleed water seepage. This paper focuses on the bleeding problems of self-flowing tailings filling paste fill with low solids concentration and investigates how the dosage of a special additive affects the seepage water bleed rate. The improvement

was studied by measuring the bleeding rate and unconfined compressive strength (UCS) of paste and analyzing the scanning electron microscope (SEM), energy dispersive spectrometer (EDS) and infrared spectroscopy (IR) of the hardened paste.

2 Experiment

2.1 Raw materials

P.O. 42.5 ordinary Portland cement and tailings from a certain mining enterprise were used in this study. Binder powder and high solidified water additives were used as cementing materials and special additives, respectively. The particle size distribution of tailings is shown in Figure 1.

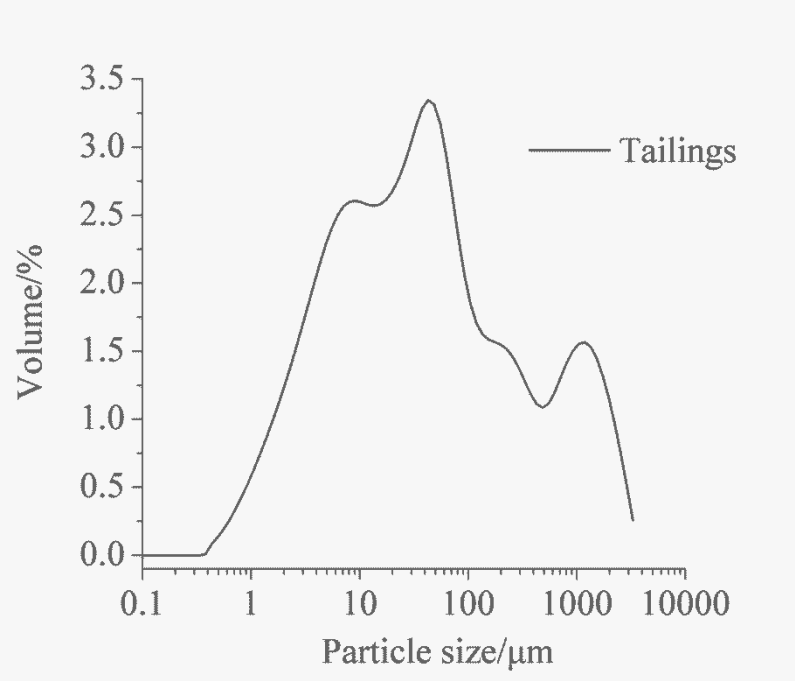

Figure 1 Particle size distribution of tailings

2.2 Test methods

Bleed Rate: After preparation (m_1), the paste was weighed, and then it was placed stationarity. At the time of 0.5, 1, 2 and 8 h, the seepage water was sucked out rapidly with a straw, and then the rest of paste was weighed (m_2). The seepage water bleed rate, α, was calculated according to Equation (1).

$$\alpha = (m_1 - m_2)/m_0 \quad (1)$$

Where m_0 is the weight of water used for the preparation of tailings filling paste.

Compressive Strength: The slurries were cast into molds with dimensions of 70.7 mm by 70.7 mm by 70.7 mm. The hardened fills were stripped from molds after curing for 2 days. Then, all the fill samples were placed in a standard curing box (at 20℃ and with 95% relative humidity). The unconfined compressive strengths of samples were measured with a WHY-600 uniaxial press machine.

Microstructure Analysis: The fills were sampled at the age of 0.5 h, 2 h, and 1 d. Then the samples were dried to terminate hydration at 30℃ for 0.5 h. The morphology of the samples was observed by SEM and the elemental analysis was conducted by EDS. The IR was analyzed by NEXUS670 instrument using KBr compression method. The scanning range was (4000~400) cm^{-1}.

3 Results and discussion

3.1 Effects of solids concentration on paste bleeding rate

High losses of bleed water are experienced for low solids concentration paste. Due to water loss, the hardened paste fill will shrink and the quality of the fill is difficult to be guaranteed. Figure 2 shows the changes of bleeding rate of tailings filling paste with solids concentration. The binder-to-tailings ratio is 1:6 (mass ratio).

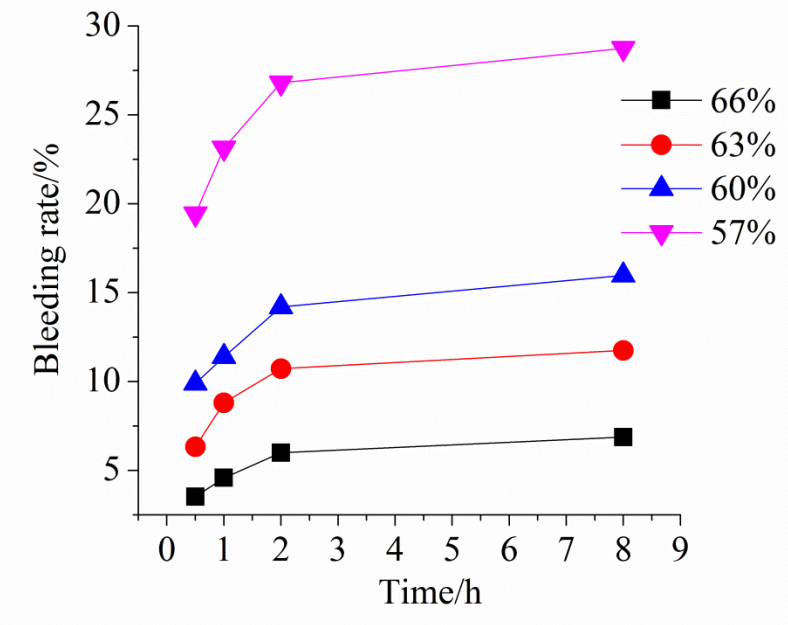

Figure 2 Effect of solids concentration on the bleeding rate of paste

It can be seen from Figure 2 that with the passage of time, the increment of paste bleeding decreases until the bleed rate reaches a steady state after 8~10 h. Since the bleed water cannot return to the paste, it results in the shrinkage of paste fill and makes it difficult for the stopes roofs to be tightly filled. With a decrease of paste solids concentration, the bleeding rate increases. When the paste concentration is reduced from 60 to 57%, the bleeding rate significantly increases from 15.98 to 28.75%. Therefore, in order to keep the paste self-flowing in the pipe, the paste concentration should not be too low.

3.2 Effects of special additive on bleeding rate and paste strength

In order to enable the self-flow as well as prevent the bleeding of the paste fill with a low solids concentration in the conveying pipe, a high solidified water additive has been developed. The dosage of the special additive is in accordance with the percentage of binder powder. Figure 3 shows the influence of the special additive on the bleeding rate of a paste sample at 8 h. The paste solids concentration is 60%. The binder-to-tailings ratio is 1:6 (mass ratio).

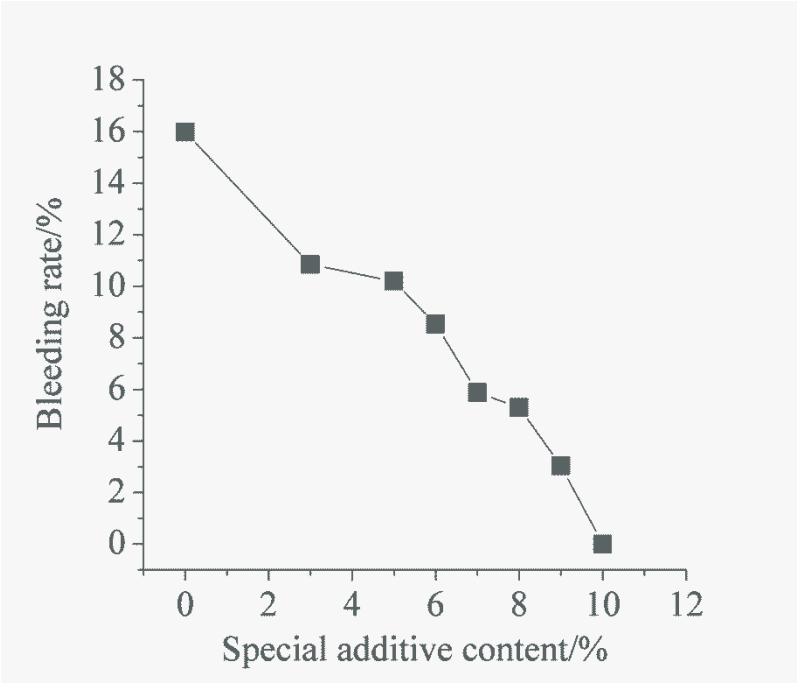

Figure 3 Effect of the special additive on bleeding rate at 8 h

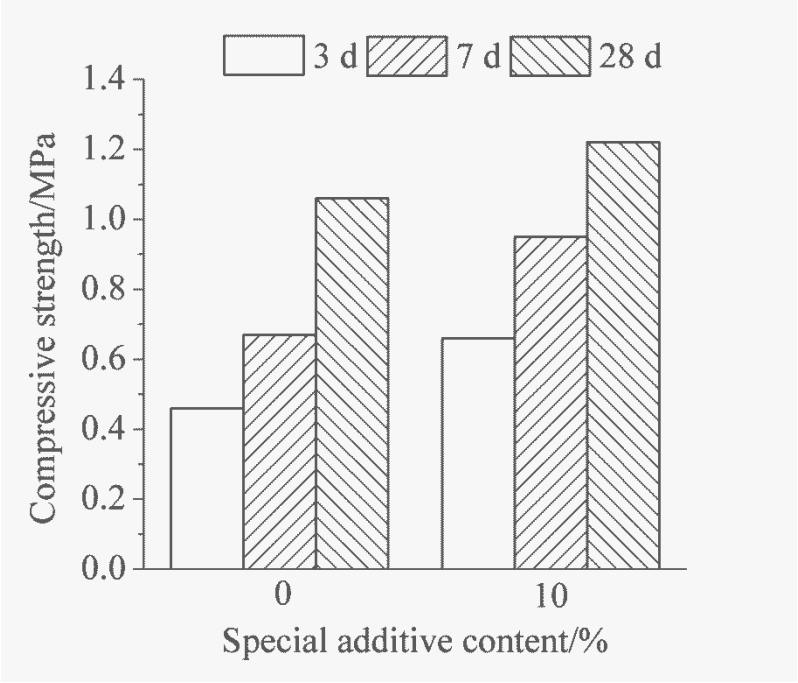

Figure 4 Effect of the special additive on compressive strength

From Figure 3, it is clear that an increase in the dosage of high solidified water additive decreases the bleed water loss at 8 h. When the dosage of the special additive accounts for 10% of the binder powder, 15.98% of the bleed water which would have been lost in the first 30 minutes has been retained as the paste enters the hardened stage.

Figure 4 shows the UCS of the filling paste with a binder-to-tailings ratio of 1:6 and a solids concentration of 60% at the age of 3, 7 and 28 days. It can be seen that when the dosage of the special additive is 10%, the UCS of the fill samples increases by 43.5, 41.8 and 15.1% at 3, 7 and 28 days, respectively, compared with that of the samples without high solidified water additive.

3.3 Effects of special additive on the microstructure of hardened paste fill

Figure 5 shows the SEM micrographs of the paste samples without special additives at the solids concentration of 60% and binder-tailings ratio of 1:6 after 30 min, 2 h, and 1 d.

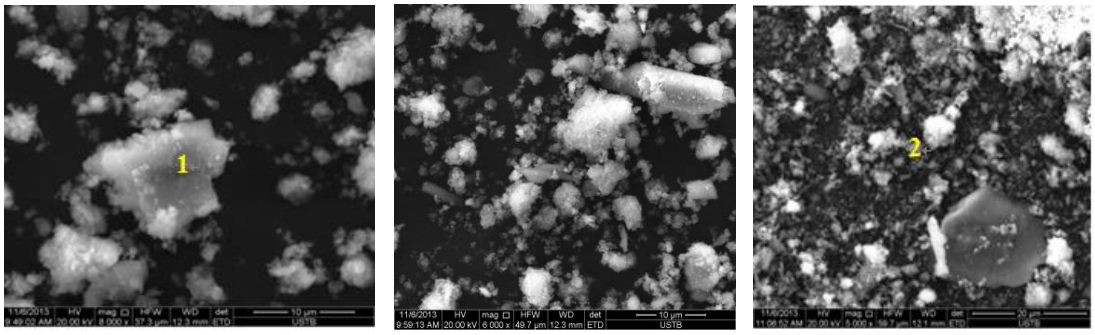

(a) (b) (c)

Figure 5 SEM micrographs of filling paste without special additives at different hydration ages; (a) 30 min; (b) 2 h; (c) 1 d

Figures 5(a) and (b) show a large distance between the particles and almost no existence of gel at 0.5 h and 2 h, indicating a large amount of free water exists in the paste. A small amount of bulk crystals and gels exist in the paste at 1 d (see Figure 5(c)). Due to the consolidation of paste and the loss of bleed water, the density of the paste increases. However, owing to the small number of hydration products, the cemented performance is poor and thus, the hardened paste fill has nearly no strength.

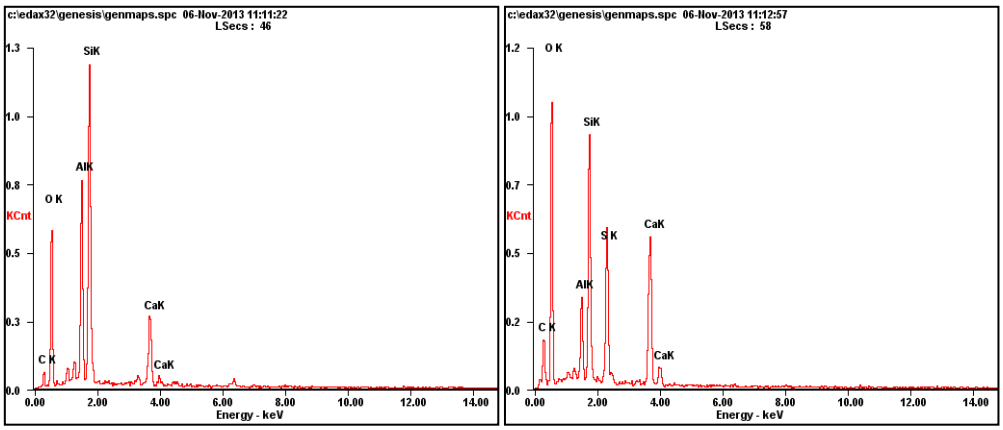

(a) (b)

Figure 6 Energy spectrums of paste from Figure 5(a) "1" and (c) "2"; (a) EDS from Figure 5(a); (b) EDS from Figure 5(c)

The energy spectrums of paste from Figure 5(a) "1" and (c) "2" are presented in Figure 6. From Figure 6(a), it is found that except for silica, alumina, calcium oxide and other components of tailings, no hydration products are generated on the particle surface after 30minutes. The presence of the four basic elements of ettringite (i.e. O, Al, S and Ca) can be found in Figure 6(b) which also confirms the existence of a small amount of needle-like ettringite in filling paste after 1 d hydration.

Figure 7 shows the SEM photographs of filling paste with special additives at 0.5 h, 2 h and 1 d at a solids concentration of 60% and the binder-to-tailings ratio of 1:6.

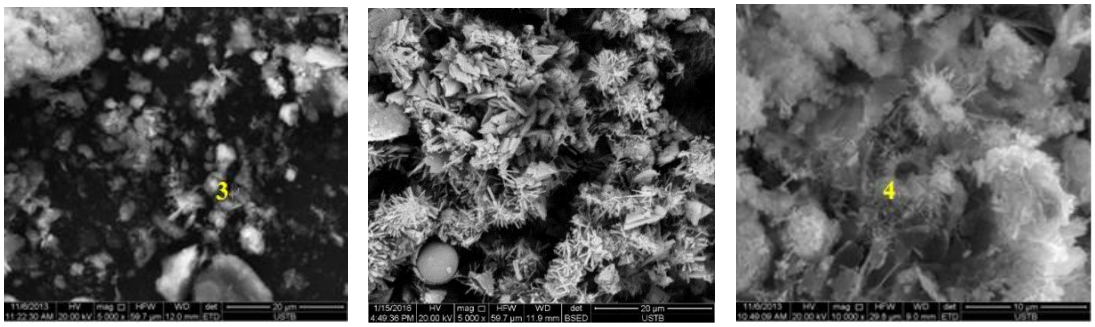

(a) (b) (c)

Figure 7 SEM photographs of filling paste with special additives at different hydration ages; (a) 30 min; (b) 2 h; (c) 1 d

A small number of hydration products are observed in the hardened filling paste at 30 minutes (see Figure 7(a)). Although some ettringite crystals and gels are generated, these crystals are relatively shorter and are not intertwined together, with most of them still being disperse. Note that the particles are relatively close, indicating the rare existence of free water. There is a relatively greater amount of gel in the hardened filling paste at 2 h (Figure 7(b)). Furthermore, needle-like ettringite crystals and crystals of calcium hydroxide with hexagonal plate exist. The crystals and gels agglomerate together. At the age of 1 d, ettringite crystals and gels are intertwined with each other, forming a denser internal structure (Figure 7(c)).

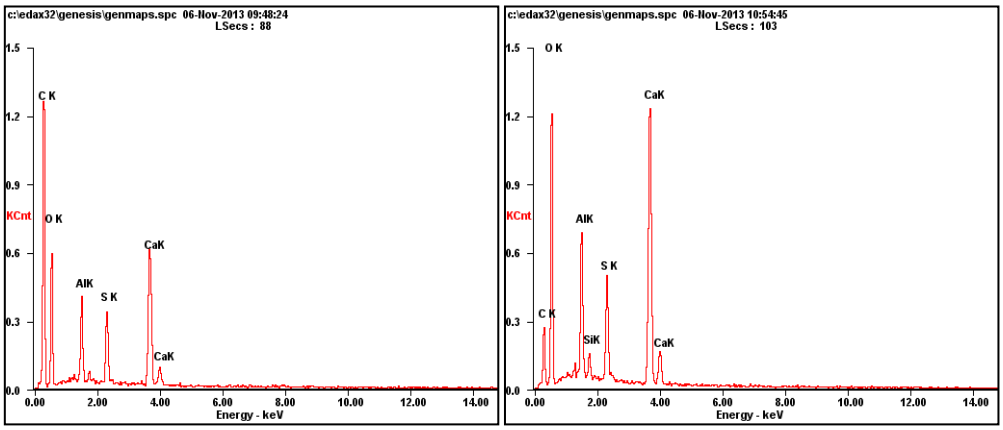

(a) (b)

Figure 8 Energy spectrums of paste from Figure 7(a) "3" and (c) "4"; (a) EDS from Figure 7(a); (b) EDS from Figure 7(c)

The energy spectrums of paste from Figure 7(a) "3" and (c) "4" are given in Figure 8. It can be seen that the four essential elements of ettringite (i.e. Ca, Al, S, and O) exist in the hardened filling paste at 30 minutes, proving that the needle-like crystals in Figure 7(a) are ettringite. The formation of ettringite greatly reduces the occurrence of paste bleeding. The peak values of Al, S, and Ca increase at 1 d (Figure 8(b)). It is elucidated that the number of hydration products increase significantly after hydrating for 1 d.

3.4 Analysis of infrared spectrum characteristics of hardened filling paste

The composition and content of the hydration products formed during the hydration process of cement-based materials can be qualitatively and quantitatively analyzed by infrared spectroscopy. The quantitative analysis of the infrared spectrum is mainly based on the measurement of absorbance, which is proportional to the concentration of the sample.

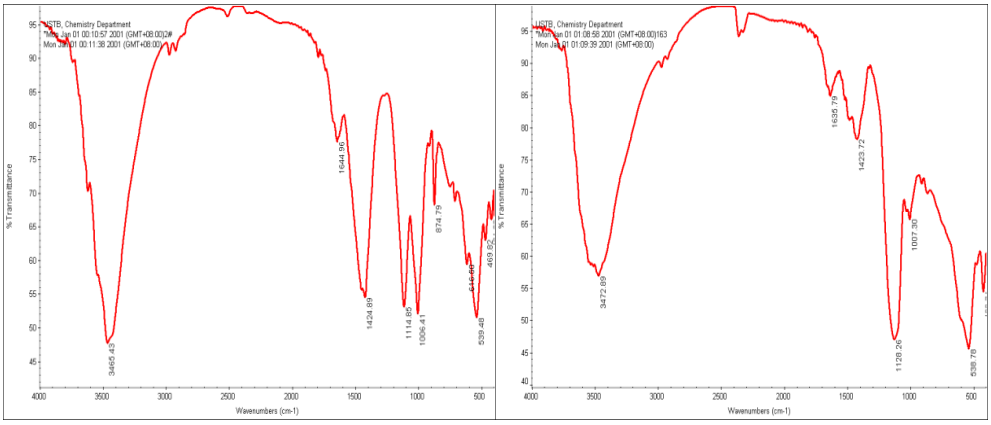

(a) (b)

Figure 9 IR spectra of 1d hardened filling paste; (a) With special additives; (b) Without special additives

The molecular structure of ettringite, $Ca_6[Al(OH)_6] \cdot 2(SO_4)_3 \cdot 26H_2O$, shows 26 water molecules combined in the form of H_2O and 6 water molecules in the form of OH. In the infrared spectrum, the absorption peak of 3640 cm^{-1} reflecting the $[OH]$ stretching vibration is less obvious, while the absorption peak of H_2O stretching vibration (about 1650cm^{-1} and 3460cm^{-1}) is significant. The strong absorption band around 1120 cm^{-1} belongs to the asymmetric stretching vibration of $[SO_4]$, and the flexural vibration of $[SO_4]$ is 610 cm^{-1}. The formation rate of ettringite in the hardened paste fill can be determined according to the change of 3640 cm^{-1} $[OH]$ absorption band and the 1122 cm^{-1} $[SO_4]$ absorption band in the infrared spectrum (Dedong, 1984). Figure 9 shows that after the incorporation of special additives, there is a shoulder at 3640 cm^{-1} in the infrared spectrum of hardened paste fill at 1 d, indicating the formation of the ettringite. By contrast, no absorption band or shoulder appears at 3640 cm^{-1} in the infrared spectrum of hardened paste fill without special additives at 1 d.

The C-S-H gel is caused by $[SiO_4]$ asymmetric stretching vibration of the absorption band located at 970, 658, and 453 cm^{-1}, which is the characteristic for identifying C-S-H. It can be seen from Figure 8(a) that the absorption band of $[SiO_4]$ at 970 cm^{-1} and 453 cm^{-1} changes with the hydration process, moving to high wave number, and these peaks are more obvious after hydrating for 1 d, indicating that the addition of high solidified water additives forms a certain amount of C-S-H gel in the filling paste after hydrating for 1 d. However, the absorption peak of C-S-H gel is not found in the infrared spectrum of the hardened filling paste without high solidified water additive after hydrating for 1 d.

4 Conclusions

In order to keep the filling paste self-flowing in the pipe, the paste solids concentration should not be too low as the decreasing the solids concentration, the bleeding rate increases. When the paste solids concentration is reduced from 60 to 57%, the bleeding rate significantly increases from 15.98 to 28.75%.

When the paste solids concentration is 60%, the binder-to-tailings ratio is 1:6, and the dosage of special additive accounts for 10% of the binder powder, the filling paste does not have any bleed water loss and the compressive strength of hardened filling paste increases by 43.5% after 3 days.

A large amount of needle-like ettringite is generated in the hardened paste after adding the special additive, and the structure becomes denser.

References

Dedong, L. 1984, 'Infrared Spectroscopic Study of Sulphoaluminate Cement', *Journal of the Chinese ceramic society*, vol. 12, no. 1, pp. 119-125.

Fall, M., Adrien, D., Celestin, J.C. 2009, 'Saturated hyedraulic conductivity of cemented paste backfill', *Minerals Engineering*, vol. 22, no. 15, pp. 1307-1317.

Fusi, L., Farina, A., Rosso, F. 2012, 'Flow of a bingham-like fluid in a finite channel of varying width: a two-scale approach', *Journal of Non-Newtonian Fluid Mechanics*, vol. 177, pp. 76-88.

Peyronnard, O., Benzaazoua, M. 2012, 'Alternative by-product based binders for cemented mine backfill: recipes optimisation using taguchi method', *Minerals Engineering*, vol. 29, pp. 28-38.

Syrakos, A., Georgiou, G.C., Alexandrou, A.N. 2013, 'Solution of the square lid-driven cavity flow of a bingham plastic using the finite volume method', *Journal of Non-Newtonian Fluid Mechanics*, vol. 195, pp. 19-31.

Wang, Y., Wang, H.J., Wu, A.X. 2011 'Research of fine tailings bleeding characteristics and influence factors', *Gold*, vol. 32, no. 9, pp. 51-54.

Wu, D., Cai, S.J. Yang, W. 2012 'Simulation and experiment of backfilling pipeline transportation of solid-liquid two-phase flow based on CFD', *The Chinese Journal of Nonferrous Metals*, vol. 22, no. 7, pp. 28-33.

Zhai, Y.G., Wu, A.X., Wang, H.J. 2011 'Threshold mass fraction of unclassified-tailings paste for backfill mining', *Journal of University of Science and Technology Beijing*, vol. 33, no. 7, pp. 795-799.

Zhang, T., Ma, M., Wang, H., 2011 'A nonlinear rheological model of backfill material for retaining roadways and the analysis of its stability', *Mining Science and Technology* (China), vol. 21, no. 4, pp. 543-546.